

# High-Resolution Spectroscopy of G191-B2B in the Extreme Ultraviolet

R. G. Cruddace<sup>1</sup>, M. P. Kowalski<sup>1</sup>, D. Yentis<sup>1</sup>, C. M. Brown<sup>1</sup>, H. Gursky<sup>1</sup>

M. A. Barstow<sup>2</sup>, N. P. Bannister<sup>2</sup>, G. W. Fraser<sup>2</sup>, J. E. Spragg<sup>2</sup>

J. S. Lapington<sup>3</sup>, J. A. Tandy<sup>3</sup>, B. Sanderson<sup>3</sup>, J. L. Culhane<sup>3</sup>

T. W. Barbee<sup>4</sup>, J. F. Kordas<sup>4</sup>, W. Goldstein<sup>4</sup>

and G. G. Fritz<sup>5</sup>

## ABSTRACT

We report a high-resolution ( $R=3000-4000$ ) spectroscopic observation of the DA white dwarf G191-B2B in the extreme ultraviolet band  $220 - 245 \text{ \AA}$ . A low-density ionised He component is clearly present along the line-of-sight, which if completely interstellar implies a He ionisation fraction considerably higher than is typical of the local interstellar medium. However, some of this material may be associated with circumstellar gas, which has been detected by analysis of the CIV absorption line doublet in an HST STIS spectrum. A stellar atmosphere model assuming a uniform element distribution yields a best fit to the data which includes a significant abundance of photospheric He. The 99-percent confidence contour for the fit parameters excludes solutions in which photospheric He is absent, but this result needs to be tested using models allowing abundance gradients.

*Subject headings:* white dwarfs—stars: individual(G191B2B)—ISM: general—circumstellar matter

---

<sup>1</sup>E. O. Hulburt Center for Space Research, Naval Research Laboratory, Washington DC 20375, U.S.A.

<sup>2</sup>Department of Physics and Astronomy, University of Leicester, Leicester LE1 7RH, U.K.

<sup>3</sup>Mullard Space Science Laboratory, University College London, Holmbury St. Mary, Dorking, Surrey RH5 6NT, U.K.

<sup>4</sup>Lawrence Livermore National Laboratory, Livermore, California 94550, U.S.A.

<sup>5</sup>Praxis Inc., 2200 Mill Road, Alexandria, Virginia 22314, U.S.A.

## 1. INTRODUCTION

White dwarfs are among the oldest objects in the Galaxy. As remnants of all stars with an initial mass  $< 8 M_{\odot}$ , they are important laboratories for study of evolutionary processes and the behavior of matter at extreme temperature and density. Study of their space and luminosity distributions helps map the history of star formation and could, in principle, determine the age of the disk, yielding an important lower limit to the age of the Universe. Further, cool white dwarfs may account for a substantial fraction of the missing mass in the galactic halo (Oppenheimer et al. 2001). However, these goals depend on our understanding of white dwarf evolution, and in particular on predictions of the cooling rates. These in turn are affected by the mass, radius and photospheric composition of the stars. Our understanding of the physical mechanisms that determine white dwarf evolution leaves unanswered several major questions. While the emergence from the AGB of two groups of white dwarfs, whose compositions are dominated by H or He, is beginning to be understood, the complex relationship between these branches, and a demonstrable temperature gap in the cooling sequence of the He-rich branch, cannot yet be explained. Determination of the photospheric He and heavy element content would provide important information on the evolutionary history of the stars. Already it has been established that significant quantities of elements heavier than He are present in the atmospheres of the hottest ( $T > 50,000$  K) white dwarfs (Barstow et al. 1998).

G191-B2B is one of the brightest and best-studied of the hot H-rich DA white dwarfs. As it lies near the top of the DA cooling sequence, measurements of its effective temperature, surface gravity and composition represent an important benchmark in the study of the whole DA sample. IUE and HST observations at high spectral resolution have made it clear, that G191-B2B falls into the group of very hot DA stars ( $T > 50,000$  K) whose atmospheres contain significant quantities of heavy elements. In particular, detections of C, N, O, Si, P, S, Fe and Ni have been reported in various studies (Bruhweiler & Kondo 1983; Sion et al. 1992; Vennes et al. 1992, 1996; Holberg et al. 1994). Such material is responsible for severe depression of the extreme ultraviolet (EUV) flux in G191-B2B at  $\lambda < 200$  Å, when it is compared with stars having pure H atmospheres, and the star has been an important target for spectroscopic EUV observations to determine the principal opacity sources. In addition, an important goal is to obtain a self-consistent model, having an effective temperature, surface gravity and composition which can fit the far ultraviolet (FUV) and EUV observations simultaneously. This would demonstrate our understanding of the star and the reliability of the model calculations, which could then be applied to other objects.

However, a complete understanding of the EUVE spectrum of G191-B2B has been

elusive. Initial attempts to match the observation with synthetic spectra failed to reproduce either the flux level or the general shape of the continuum (see Barstow et al. (1996)), as the model contained insufficient Fe and Ni lines. Consequently  $\sim 9$  million predicted lines were added to the few thousand with measured wavelengths, yielding a self-consistent model able to reproduce the EUV, FUV and optical spectra (Lanz et al. 1996). However, good agreement could be achieved only by including a significant quantity of He, either in the photosphere or in an ionised interstellar component. Unfortunately, due to the limited resolution of EUVE ( $\sim 0.5$  Å) in the He II Lyman series band, the He contribution could not be detected directly. More recently, it has been shown that photospheric heavy elements may not be distributed homogeneously in the radial direction, so that more complex stratified structures should be considered. This approach has yielded a good fit of model atmospheres to observational data across the soft X-ray, EUV and FUV bands (Barstow, Hubeny & Holberg 1999; Dreizler & Wolff 1999). Important progress has been made also in incorporating radiative levitation and diffusion self-consistently into the calculations (Dreizler & Wolff 1999; Schuh, Dreizler & Wolff 2001). The need for a He contribution is reduced in these stratified models but not eliminated. We present the results of a search for the He II component in the EUV spectrum of G191-B2B, using the J-PEX (Joint Astrophysical Plasmadynamic Experiment) high-resolution EUV spectrometer. This spectrum was obtained by J-PEX after launch by a sounding rocket in February 2001.

## 2. The J-PEX High Resolution EUV Spectrometer

The J-PEX spectrometer, described by Cruddace et al. (in preparation), is a slitless, normal-incidence instrument employing figured spherical gratings in a Wadsworth mount. The optic comprises four ion-etched laminar gratings with a groove density of  $3600 \text{ g mm}^{-1}$  and a focal length of 2.0 m. The gratings are coated with a  $\text{Mo}_5\text{C}/\text{Si}/\text{MoSi}_2$  multilayer designed to operate in the band  $220 - 245$  Å, and are optimised to suppress zero order and to yield maximum efficiency in first order at 235 Å. At this wavelength the spectrometer achieves an effective area of  $3.0 \text{ cm}^2$ . The design specification for the spectral resolving power ( $R$ ) in flight is 4980, which includes the effect of a pointing uncertainty of 1 arcsec. Calibration of  $R$  was hindered by thermal deflections in the spectrometer, caused by detector heating over long exposure times, and consequently the average measured resolving power was 2750, yielding an estimate for inflight resolving power of 2600. However the problem encountered in calibration should have a much smaller effect during a flight lasting only 5 minutes. Therefore we can only set reasonable bounds to the resolving power in flight, namely  $3000 < R < 4000$ . This uncertainty is taken into account in analysis of the flight data. J-PEX was launched by a NASA Black Brant IX sounding rocket (NASA 36.195DG)

at 05.45UT on 22 February 2001. The payload completed its mission successfully, during which it observed the target G191-B2B for 300 seconds.

### 3. Data Reduction and Analysis

The spectra of the four gratings were recorded independently by the focal-plane detector. In Cruddace et al. (in preparation) we describe how the positions of photon events in each spectrum were corrected for ACS drift and jitter, and the wavelength of each spectrum was calibrated. The events were summed in bins of width  $0.024 \text{ \AA}$ , before being superposed to yield one spectrum. The bin width was chosen to oversample the data by a factor 2.4 in comparison with the resolution at  $R = 4000$ , so as to minimise loss of information during superposition. The final spectrum, in which the signal-to-noise ratio (S/N) has been maximised by increasing the bin size to  $0.048 \text{ \AA}$ , is shown in Figure 1. The average S/N per bin was 5.0. The background count-rate in the detector field during the observation was  $4.2 \text{ cts s}^{-1}$ , sufficiently low that the spectra were essentially free of background. Therefore the error bars in Figure 1 have been assigned assuming Poisson statistics. The spectrum contains one flaw caused by the pointing on target, in which data above  $\sim 239 \text{ \AA}$  was lost in two of the spectra. Thus only half the instrument effective area was used in this region, in which accordingly we have increased the bin width to  $0.096 \text{ \AA}$ .

We have compared the observed spectrum with the predictions of a model, in which the white dwarf atmosphere has a homogeneous composition and the flux is absorbed by H I, He I and He II in the interstellar medium (ISM). Although stratified atmosphere models are more successful in reconciling spectra of G191-B2B in the EUV and FUV bands (Barstow and Hubeny 1998; Barstow, Hubeny & Holberg 1999), the homogeneous models are adequate for the relatively narrow J-PEX waveband, and give a useful baseline for comparison with abundance measurements made in other studies. The analysis technique has been described extensively in earlier papers (e.g. Lanz et al. 1996), and we give here only a brief overview. The XSPEC software was used to fold model spectra through the J-PEX instrument response, and as we were dealing with a spectrum having a small number of counts per bin, the best match between model and data was obtained by minimisation of the Cash statistic (Cash 1979). This does not assign an absolute value to the goodness of fit, but does allow uncertainty ranges to be determined for each free parameter.

The model spectra, based on work reported by Lanz et al. (1996) and Barstow, Hubeny & Holberg (1998, 1999), were calculated using the non-LTE code TLUSTY (Hubeny & Lanz 1995). For this initial analysis, we fixed the stellar temperature and surface gravity ( $T_{\text{eff}} = 54,000 \text{ K}$ ,  $\log g = 7.5$ ) at the grid points closest to the values determined using the

Balmer and Lyman lines (Barstow, Hubeny & Holberg 1998). Apart from the He abundance, which was allowed to vary freely between the grid limits of  $10^{-4}$  and  $10^{-6}$ , the heavy element abundances were fixed at values determined in earlier homogeneous-model analyses of G191-B2B ( $C/H = 4.0 \times 10^{-7}$ ,  $N/H = 1. \times 10^{-7}$ ,  $O/H = 9.6 \times 10^{-7}$ ,  $Si/H = 3.0 \times 10^{-7}$ ,  $P/H = 2.5 \times 10^{-8}$ ,  $S/H = 3.2 \times 10^{-7}$ ,  $Fe/H = 1.0 \times 10^{-5}$ ,  $Ni/H = 5.0 \times 10^{-7}$ ).

The value taken for  $Fe/H$  lies between limits established by FUV ( $2.4 \times 10^{-6}$ , Vennes & Lanz (2001)) and EUV ( $3-4 \times 10^{-5}$ , Barstow, Hubeny & Holberg (1999)) analyses. The effect of  $Fe/H$  in the 225 – 245 Å band is to change the level of the overall spectrum, and we have verified that this does not affect the conclusions reached in our analysis. The ISM H I and He I column densities were fixed at values obtained from analysis of the broader-band, lower-resolution EUVE spectrum (Barstow, Hubeny & Holberg 1999): H I =  $2.15 \times 10^{18} \text{ cm}^{-2}$ , He I =  $2.18 \times 10^{17} \text{ cm}^{-2}$ . The parameters varied during the fit were the column density of He II in the line-of-sight ( $N_{\text{HeII}}$ ) and the photospheric He abundance ( $n_{\text{He}}$ : measured by numbers of nuclei). For this fit, the data were summed in bins of width 0.060 Å, equivalent to  $R = 4000$ . Given the uncertainty in the resolving power (section 2,  $R = 3000 - 4000$ ), the fits were performed also for lower values of  $R$ , but yielded no significant change in the results presented below in section 4. The best fit to the data, shown by the red line in Figure 1, was obtained for  $N_{\text{HeII}} = 5.97 \times 10^{17} \text{ cm}^{-2}$  and  $n_{\text{He}} = 1.60 \times 10^{-5}$ , and in Figure 2 we show the 1, 2, 3, 5 and 10 sigma contours for the two parameters. The 3 sigma contour is the locus on which  $\chi^2$  exceeds the minimum by 11.8, and within which the parameter confidence level is greater than 99.7 percent. We use this contour to derive 99-percent confidence limits of  $5.76 - 6.18 \times 10^{17} \text{ cm}^{-2}$  for  $N_{\text{HeII}}$  and  $1.31 - 1.91 \times 10^{-5}$  for  $n_{\text{He}}$ .

#### 4. Discussion

The good agreement between the best-fit model and the data in Figure 1 is striking, for example at the prominent absorption feature at 233.5 Å produced by a cluster of O IV lines. Many other features are present, which are mainly blends of large numbers of Fe V and Ni V lines. The broad features between 227 and 232 Å are a characteristic of the overlapping series of interstellar He II absorption lines superposed on a continuum. This is shown more clearly in the upper panel of Figure 3, an expanded view of the region 226 – 232 Å in Figure 1. Taken with the strong depression of the flux below 227 Å this is strong evidence that interstellar He II is present along the line of sight. Conclusive proof is obtained when the data are fitted by a model in which  $N_{\text{HeII}}$  is set to zero. The degradation of the fit is evident in the lower panel of Figure 3, particularly in the region below 229 Å. Further, in this case the best-fit value of  $8.0 \times 10^{-5}$  for  $n_{\text{He}}$  is about four times the upper limit we obtained from

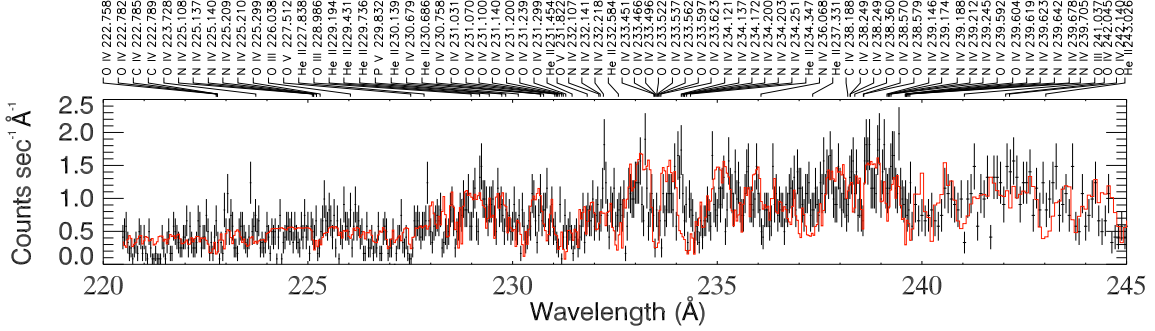


Fig. 1.— High resolution EUV spectrum of G191-B2B, obtained with the J-PEX spectrometer in the waveband 221 – 244 Å. All data points have error bars. The red histogram is the best-fit model of the star and ISM. The strongest predicted lines of He, C, N, O, and P are labeled with their ionization state and wavelength. Lines of Fe and Ni, too numerous to include here, account for some unlabelled individual features and broader absorption structures.

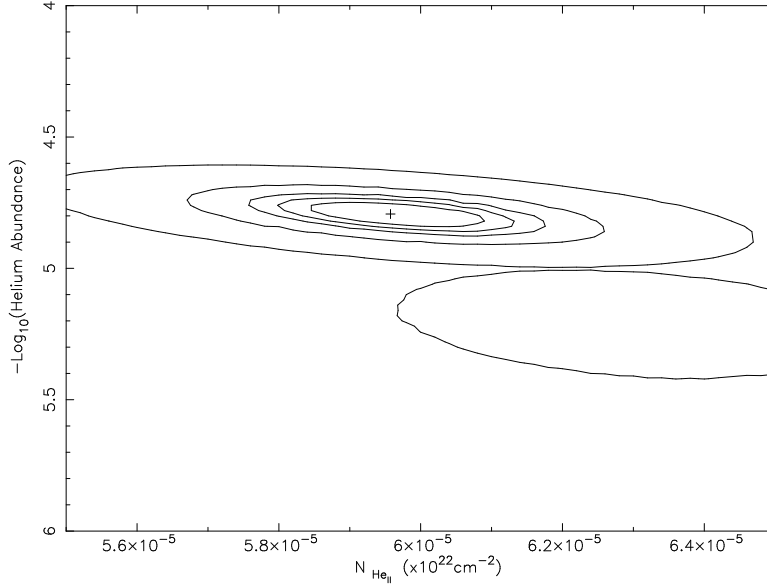


Fig. 2.— The 1, 2, 3, 5 and 10 sigma contours for the two parameters varied in fitting a uniform abundance white dwarf atmosphere model to the measured spectrum of G191-B2B. The 3 sigma contour corresponds to a confidence level of 99.7 percent. The secondary contour at 10 sigma locates a weak secondary minimum in the  $\chi^2$  distribution.

the absence of detectable He II at 1640 Å in the STIS spectrum of G191-B2B. On the other hand, the best-fit model in the upper panel of Figure 3, in which  $n_{\text{He}} = 1.6 \times 10^{-5}$ , is consistent with the STIS limit.

The best-fit He II column density of  $5.97 \times 10^{17} \text{ cm}^{-2}$  implies a He ionization fraction, based on EUVE measurements of the He I column density, of  $\sim 0.73$ . This is substantially higher than the typical range of 0.25-0.50 in the local interstellar medium (LISM; e.g. Barstow et al. 1997). However, a possible circumstellar (CSM) component has been identified recently through analysis of the CIV absorption line doublet (1548.202 and 1550.774 Å) in the STIS FUV spectrum of G191-B2B (Bannister et al. 2001). Therefore some of the He II detected in the J-PEX spectrum may be circumstellar, although the fraction would have to be at least one third to bring the interstellar component within the LISM range. The known LISM and CSM components are separated by  $\sim 8 \text{ km s}^{-1}$ , and therefore could not be resolved by J-PEX.

The photospheric absorption line at 243.026 Å is predicted to be the strongest in the J-PEX waveband. Unfortunately this lies in a region of reduced exposure (Section 3), and Figure 1 shows no feature in the measured spectrum at this wavelength. However, the depth of the predicted line is similar to the magnitude of the statistical errors for the data points, yielding only a very weak constraint on the possible He abundance. A weak absorption line is seen at the position of He II 237.331 Å but likewise the photon statistics do not allow a significant detection.

The above discussion of the column density of ISM/CSM He II, and the evidence for photospheric He, is underpinned by the good agreement between the homogeneous stellar atmosphere models and the observational data, as shown by the good correspondence between predicted and observed features in Figure 1 and the upper panel of Figure 3. However, closer inspection also reveals several significant features present in the observed but not in the synthetic spectrum, for example at 229.3 and 231.2 Å. This indicates that the model atmosphere is incomplete and that other elements should be included in addition to C, N, O, Si, P, S, Fe and Ni.

## 5. Conclusions

We have presented our first analysis of the high-resolution EUV spectrum of G191-B2B obtained with the J-PEX spectrometer, which has the highest resolving power (3000-4000) achieved so far in the EUV and X-ray wavebands. The results show conclusively that ionised He is present along the line-of-sight, and yield a column density of  $5.97 \times 10^{17} \text{ cm}^{-2}$ . However

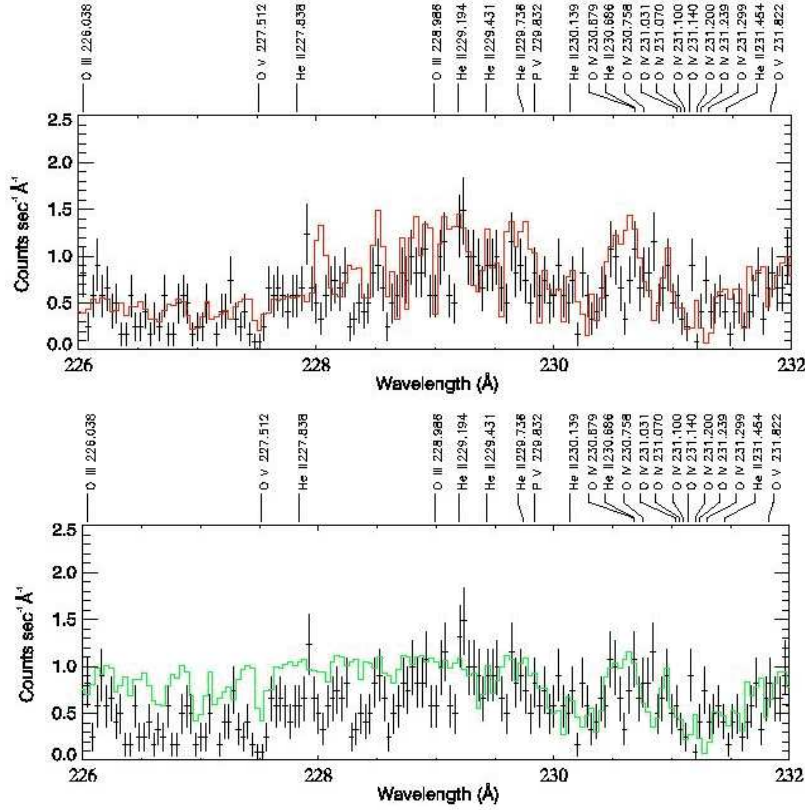


Fig. 3.— Upper panel: Expanded view of the J-PEX spectrum of G191-B2B in the wavelength range 226 – 232 Å spanning the He II Lyman series limit. The red histogram is the best-fitting model of the stellar atmosphere and absorption in the ISM.

Lower panel: Expanded view of the J-PEX spectrum of G191-B2B in the range 226 – 232 Å but this time showing the best fit, traced by the green histogram, of a model in which absorption by interstellar and circumstellar He has been removed.



if this is all interstellar, the measured column density yields an estimated He ionisation fraction significantly higher than is typical of the LISM. Some of this material may be associated with a newly discovered circumstellar component, but further investigation is necessary to demonstrate whether this is plausible.

The white dwarf model which best fitted the data included a significant abundance,  $1.6 \times 10^{-5}$ , of photospheric He, and at the 99-percent confidence level we could exclude models containing no photospheric He. However, we caution that a simple model, in which elements are distributed uniformly in the atmosphere, was used in this analysis, and further work with models in which stratification of elements is allowed, and taking greater advantage of other G191-B2B observations, is needed to verify or disprove our result.

The Naval Research Laboratory was supported in this work by NASA under the grant NDPR S-47440F, and by the Office of Naval Research under NRL Work Unit 3641 (Application of Multilayer Coated Optics to Remote Sensing). The University of Leicester and the Mullard Space Science Laboratory acknowledge the support they received for this project from the Particle Physics and Astronomy Research Council in the U. K.

## REFERENCES

- Bannister, N. P., Barstow, M. A., Holberg, J. B., & Bruhweiler, F. C. 2001, Proceedings of the 12th European White Dwarf Workshop, Eds. J. L. Provencal, H. L. Shipman, J. MacDonald & S. Goodchild, ASP Conference Series, 226, 105
- Barstow, M. A., Hubeny, I., Lanz, T., Holberg, J. B., & Sion, E. M. 1996, in *Astrophysics in the Extreme Ultraviolet*, Eds. C. S. Bowyer & R. F. Malina, Dordrecht: Kluwer, 203
- Barstow, M. A., Dobbie, P. D., Holberg, J. B., Hubeny, I., & Lanz, T. 1997, MNRAS, 286, 58
- Barstow, M. A., et al. 1998, MNRAS, 264, 16
- Barstow, M. A., & Hubeny, I. 1998, MNRAS, 299, 379
- Barstow, M. A., Hubeny, I., & Holberg, J. B. 1998, MNRAS, 299, 520
- Barstow, M. A., Hubeny, I., & Holberg, J.B. 1999, MNRAS, 307, 884
- Bruhweiler, F. C., & Kondo, Y. 1983, ApJ, 269, 657
- Cash, W. 1979, ApJ, 228, 939

- Dreizler, S., & Wolff, B. 1999, A&A, 348, 189
- Holberg, J. B., Hubeny, I., Barstow, M. A., Lanz, T., Sion, E.M., & Tweedy, R. W. 1994, ApJ, 425, L105
- Hubeny, I., & Lanz, T. 1995, ApJ, 439, 875
- Lanz, T., Barstow, M. A., Hubeny, I., & Holberg, J. B. 1996, ApJ, 473, 1089
- Oppenheimer et al. 2001, Science, 282, 698
- Schuh, S., Dreizler, S., & Wolff, B. 2001, Proceedings of the 12th European White Dwarf Workshop, Eds. J. L. Provencal, H. L. Shipman, J. MacDonald & S. Goodchild, ASP Conference Series, 226, 79
- Sion, E. M., Bohlin, R. C., Tweedy, R. W., Vauclair, G. P. 1992, ApJ, 391, L29
- Vennes, S., Chayer, P., Thorstensen, J. R., Bowyer, S., & Shipman, H. L. 1992, ApJ, 392, L27
- Vennes, S., Chayer, P., Hurwitz, M., & Bowyer, S. 1996, ApJ, 468, 989
- Vennes, S., & Lanz, T. 2001, ApJ, 553, 399